aci avances en ciencias e ingenierías

Artículo/Article
Sección A/Section A
Vol. 15, nro. 1
ID: 2780

Demonstrating the feasibility of testing microscopic acausality at the LHC with CMS open data

Jonathan Sanchez[1]*

Universidad San Francisco de Quito, Colegio de Posgrados, Maestría en física de altas energías, Quito, Ecuador, https://orcid.org/0000-0002-7302-5968

*Jonathan Joel Sánchez Jácome, email: jjsanchezj@outlook.com

Demostrando la viabilidad de estudiar la acausalidad microscópica en el LHC con datos abiertos de CMS

Abstract

In this work, we describe the feasibility to reconstruct and measure acausal vertices that could arise from Lee Wick standard model processes. Using open data from the CMS experiment, we identify measurable wrong displaced vertices associated to acausal-like decays predicted by the Lee Wick model. The signal considered is the pair production of Lee Wick electrons due to its favorable cross-section. We estimated that the Lee Wick electron mass is equal to 200 GeV, because it can satisfy detector resolution limitations. The final state consists of one electron and a pair of jets emerging from a wrong displaced vertex for each of the Lee Wick electrons. We detail the method used to reconstruct wrong displaced vertices with the given topology. We also define a new quantity, the parallelity ($\kappa_{\parallel}$), to better distinguish wrong displaced vertices. We compare the histograms of parallelity between events of simulated backgrounds, experimental data from Run 1, and the signal. An asymmetry in the parallelity distribution suggests the capability of distinguishing acausal decays if ever present.

Keywords: Finite theories, Lee Wick standard model, causality violation, wrong displaced vertex, CMS Open Data, parallelity

Resumen

Este trabajo describe la posibilidad de reconstruir y observar vértices acausales originados del modelo estándar de Lee Wick. Haciendo uso de la base de datos abiertos del experimento CMS fue posible identificar vértices erróneamente desplazados predichos por el modelo de Lee Wick. La señal considerada se origina de la producción de pares de electrones de Lee Wick gracias a su favorable sección eficaz. El estudio se realizó con una masa del electrón de Lee Wick igual a 200 GeV, ya que supera las limitantes de resolución del experimento. El estado final consiste en un electrón y un par de jets originados de cada uno de los electrones de Lee Wick. Se detalla el método utilizado para reconstruir vértices erróneamente desplazados con la topología mencionada. Además se define una nueva cantidad, la paralelidad ($\kappa_{\parallel}$), para distinguir vértices erróneamente desplazados de mejor manera. Comparamos los histogramas de parelelidad entre eventos de backgrounds simulados, datos experimentales de la Corrida 1 y la señal. Una asimetría en la distribución de paralelidad sugiere la posibilidad de distinguir decaimientos acausales si existiesen.

Editado por / Edited by:
Eva O.L. Lantsoght

Recibido / Received:
25/07/2022

Aceptado / Accepted:
17/02/2023

Publicado en línea / Published online:
15/05/2023

DOI: https://doi.org/10.18272/aci.v15i1.2780

Palabras clave: Teorías finitas, modelo estándar de Lee Wick, violación de la causalidad, vértice erróneamente desplazado, Datos abiertos de CMS, paralelidad

It is usually hard to challenge ideas that serve as the foundation of physics. Causality, i.e., the notion that an effect is preceded by a cause, is a vivid example. State-of-the-art research machines, like the Large Hadron Collider (LHC) [1] at the CERN laboratory in Switzerland, offer a unique opportunity to test the notion of causality, not at the macroscopic level but at the microlevel in physics.

Known limitations of the Standard Model (SM) of particle physics [2] have encouraged physicists to formulate diverse extensions of this theory. One of those ideas, on which some of the least tested versions are based, is known as the Lee-Wick (LW) Standard Model (LWSM)[3]. It is founded on the finite theory of quantum electrodynamics model proposed by Lee and Wick [4]. Among other consequences, the model predicts an observable that could change the understanding of causality in the realm of fundamental interactions [5].

In the LWSM re-normalization process, each standard field is paired to an LW field. In the context of the by-products of high-energy hadronic collisions, those LW fields are associated to fast decaying, heavier particles, which could microscopically violate causality. In a causal resonant decay, after a particle is produced in the so-called primary vertex, it travels a certain distance, to a secondary vertex (SV), before decaying into other particles (Figure 1.A). On the other hand, in the case of LW resonances, their final decay products appear at the same time (or before) the resonance was generated, as if the LW field would have propagated backwards in time [6]. These decays have a *wrong displaced vertex* (WDV) that can be distinguished because the total momentum of the final particles at the SV seems to point towards the collision spot [7], as depicted in Figure 1.B. For a macroscopic observer, the time differences between these two types of events are impossible to measure, yet they could be distinguished by observing their WDV topology.

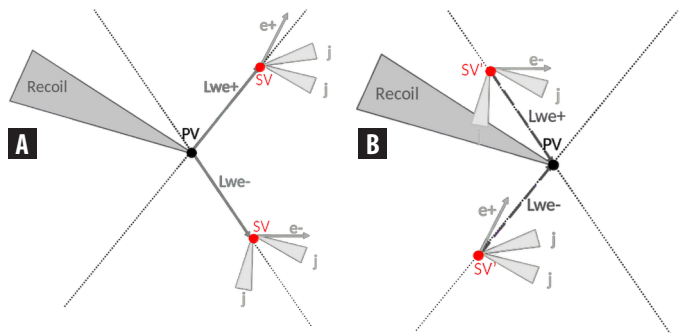

Figure 1: A. Resonant decay as if LW-electrons (Lwe±) were produced in the primary vertex (PV) and causally decay at the secondary vertex (SV) into electrons (e±) and jets (j); **B.** Acausal resonant decay as if LW-electrons (Lwe±) were produced in the PV and acausally decay at the wrong displaced secondary vertex (SV') into electrons (e±) and jets (j).

DOI: https://doi.org/10.18272/aci.v15i1.2780

Theoretical results suggest that it would be possible to test this acausal behaviour using collisions data from the LHC experiment. To the best of our knowledge, direct tests for these ideas have never been tried out. This is perhaps due to the small cross section of these processes and the large amounts of data needed. In this work, we used CMS open data to test the feasibility of carrying out these studies even if the volume of data is not yet sufficient to search for LW particles. These data were taken by the CMS experiment, one of the largest detectors at the LHC, during the so-called Run 1 period. Details about the CMS detector can be found elsewhere [8]. Among other characteristics, CMS had, at the time, a spatial resolution of about 0.02 mm for the determination of primary and secondary vertices. This feature im- posed the main restriction to this investigation.

The best approach to overcome the experimental limitations is to study processes of LW-electrons ($\ell^{e\pm}$) emerging from the Neutral Current (NC) sector of the LWSM [7],

$$\begin{aligned}\mathscr{L}_{NC} = -Z_\mu [& g_Z^{e_L}(\bar{e}_L \gamma^\mu e_L - \bar{\tilde{\ell}}^e_{eL}\gamma^\mu \tilde{\ell}^e_{eL}) + g_Z^{e_R}(\bar{e}_R\gamma^\mu e_R - \bar{\tilde{\ell}}^e_{eR}\gamma^\mu \tilde{\ell}^e_{eR}) \\ & + (g_Z^{e_L} - g_Z^{e_R})\frac{m_e}{M_\ell}(\bar{e}_R\gamma^\mu \tilde{\ell}^e_{eR} - \bar{\tilde{\ell}}^e_{eR}\gamma^\mu e_R)],\end{aligned} \tag{1}$$

where the suffix R (L) indicates the right-handiness (left-handiness) and $g_Z^{e_{R,L}}$ are the coupling constants between Z bosons and SM electrons. These particles, created in pairs, would later decay into a pair of SM electrons and Z bosons, namely, $Z \to \ell^{e+}\ell^{e-} \to e^+ Z e^- Z$.

Similar to reference [7], we calculated the Feynman rules and the average flight distances λ for this process with the Mathematica [9] package named FeynRules [10]. A summary of the values of λ , which are close to the minimum resolution of the CMS detector, are shown in Table 1 for different values of LW electron mass. The cross sections (σ) for each mass value, which were calculated from simulated events in Madgraph 5 [11] for proton-proton collisions at 8 TeV, are shown in the same table. We used Pythia 8 [12] for the simulation of the showering and hadronization processes, after restricting the Z-boson decays to the hadronic channel ($Z \to jj$). The final state is characterized by the presence of a pair of energetic electrons and 4 jets (j) coming from a displaced vertex, $\ell^{e+}\ell^{e-} \to e^+e^- jjjj$. Finally, the interaction of the decay products with the CMS sub-detectors was simulated using CMS software (CMSSW) [13] built-in tools [14]. Further descriptions are made with LW electron mass equal to 200 GeV, because of being the best candidate considering cross section and average flight distance.

Table 1. Calculated cross-section (σ) and fly distance (λ) for each mass value, $M_\ell = 200, 300, 400, 500$ GeV.

M_ℓ(GeV)	σ (fb^{-1})	λ (mm)
200	5.97	2.70765e-02
300	0.96	1.64300e-02
400	0.23	1.21212e-02
500	0.06	9.65243e-03

DOI: https://doi.org/10.18272/aci.v15i1.2780

Causally decaying vertices (Figure 1.A) only differ from WDV events (Figure 1.B) in the direction of the displacement vector from the PV to the SV $\overrightarrow{PVSV}$. A *parallelity* ($\kappa_{||}$) variable was defined, for the first time, as the scalar product between $\overrightarrow{PVSV}$ and the total momentum of the decaying products, $\vec{P}_{total}$. This quantity was used as the discriminator between causal decays, with mostly ($\kappa_{||}$) > 0, and LW-decays, which tend to have values of $\kappa_{||} < 0$. Because of conservation laws, we cannot simulate proper WDV decays, so we simulated our particles as causal decaying resonances. For this reason, we selected the opposite of $\kappa_{||}$ when the vertex comes from our signal.

To assess the feasibility of distinguishing events with displaced vertices, we look for candidate events with two jets and one energetic electron in the final state and study their $\kappa_{||}$ distribution. The two experimental datasets used ([15] and [16]) are characterized by the presence of events with at least two energetic photon- or electron-like (egamma) particles, corresponding to total integrated luminosity of 4.412 and 7.055 fb^{-1}, respectively. To consider background processes that could give similar signatures, we use the following simulated datasets: Drell-Yang (DY) [17], top quark pair production (TTbar) [18], and W boson production in association with jets (WJets) [19, 20, 21], corresponding to cross-sections of 3503.7, 225.2 and 1.75×10^{-1} pb, respectively. The background, which originated from quantum chromodynamic (QCD) processes, was estimated from a region orthogonal to our signal. We fitted QCD to better match background and experimental data when the most energetic egamma particles have the same charge. The fitting was then extrapolated to the region that contains our signal.

In a first stage for event selection, collisions were subject to pass a trigger that requires the presence of two highly isolated and mild shower-shaped egamma objects with transverse momentum over 36 GeV for the leading particle, and 22 GeV for the subleading one. Additionally, we require the egamma particles to be electrons and the presence of 4 jets with transverse momentum greater that 15 GeV. This selection requirement was named Trigger Filtering (TF). Details of the selection can be found in studies with SV reconstruction from leptons [22].

After the initial filtering, an Object Selection (OS) requirement was implemented. There, the electrons' minimum transverse momentum was tuned up to 40 GeV and 25 GeV. This guarantees a trigger efficiency of 99% [23]. Tracks associated to electrons are also required to match the high quality selection described in [22]. Additionally, at least 4 selected jets in the event must be from hadronic origin and have two or more constituents and a transverse momentum greater than 20 GeV. Details for this selection can be found in a previous study with SV reconstruction from hadronic jets [24]. Additionally, we required an electromagnetic jet energy fraction less than 0.6 to filter out mix of jets and electrons, more common in our topology than in others.

We also apply a Signal (SG) filter. We require that events must contain selected electrons of opposite charge. It is also required that the electron-jet structure follows this geometrical property: that the difference between the angular distance from the electron to the closest jet (ΔR_1) and the distance from the electron to the second closest jet (ΔR_2) be (ΔR_2) be $|\Delta R_1 - \Delta R_2| < 0.2$. Here, $\Delta R = \sqrt{\Delta\phi^2 + \Delta\eta^2}$ is defined by the difference in the azimuthal angles (φ) and the pseudorapidities (η) of the objects.

DOI: https://doi.org/10.18272/aci.v15i1.2780

This spatial topology of electrons and jets was most commonly found in the acausal signal than in the background processes.

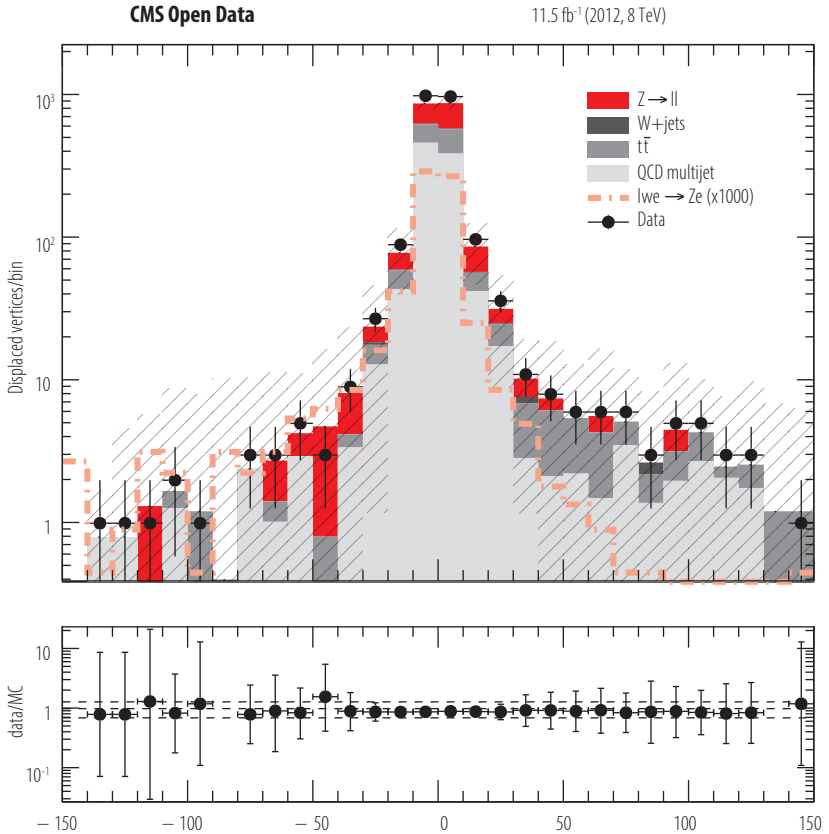

Figure 2. Parallelity κ , for reconstructed displaced vertex from a pair of jets plus one electron is the scalar product between the total momentum of the objects at that vertex and the displacement vector of the SV. Background processes are shown in solid-colored histograms, while a signal example (blown up 1000 times) is drawn with a green dotted line. Black solid dots rep resent collisions data with the bars being their statistical uncertainty. Hashed regions represent the systematic uncertainties considered. An asymmetry between background processes and the signal is evident.

The SV were reconstructed using the combination of selected electrons and any pair of jets that happen to reconstruct and invariant mass between 80 and 160 GeV. The total amount of tracks resulting from this combination was then fed to an SV reconstruction algorithm (SVRA) described in [24]. The SVRA forces any possible pair of tracks to a vertex fitting algorithm. Only SV with an adequate fitting chi-squared normalized to the number of degrees of freedom ($\chi^2_{norm} < 5$) are selected. If any pair of SV share one or more tracks, the combined set of tracks is refitted to a new SV′. This process is repeated until none of the selected SV share tracks or there are no left well-fitted

DOI: https://doi.org/10.18272/aci.v15i1.2780

vertices. Resulting SV′ are then selected to guaranty they are well fitted, composed of at least 5 tracks, and follow other geometrical considerations as described in reference [24]. We also calculated the $\kappa_{\parallel}$ value for each SV that contains the selected electrons. The comparative distributions for values of $\kappa_{\parallel}$ are found in Figure 2. It is evident that, while SM model contributions (solid colors) show a rather symmetrical histogram, the signal histogram (in green dotted line) leans towards negative values of $\kappa_{\parallel}$.

For the final WDV selection criteria (WDVC), we require events to have at least one adequately-selected WDV: the WDV must be associated to one electron track; every SV associated to the same electron must have a separation transverse to the collision axis $\vec{PVSV}^{t} > 0.02$ mm; and the total transverse momentum $\vec{P}^{t}_{total} > 20$ GeV.

Systematic uncertainties were estimated from the object and event selection comparable to the literature and can be visualized in Figure 2 as hashed bands. The uncertainty in the trigger efficiency was extracted from reference [23]. Uncertainties in electron energy and tracking alignment were inferred from [22]. Jet energy resolution and vertex reconstruction are comparable to reference [24], yet methods are not exactly the same, so we conservatively consider uncertainties of 3% and 18% respectively. Underlying events and integrated luminosity uncertainties are comparable to those found in reference [23]. A summary of the values can be found in Table 2.

Table 2. Systematic uncertainties for the selected objects that could mostly affect the value of parallelity calculation $\kappa_{\parallel}$.

Source	Uncertainty (%)
Vertex reconstruction	18
Jet energy resolution	3
Electron energy resolution	1
Underlying event	3
Tracker misalignment	2
Integrated Luminosity	3
Trigger efficiency	1

In conclusion, we have confirmed the feasibility of identifying WDV decays in events containing a pair of energetic electrons and 4 jets in CMS open data. Considering the upgrades that have taken place for the LHC experiments, including CMS, and the greater amounts of data that will be collected in upcoming years, we believe that the WDV method described in this study, together with a refined handling of systematic uncertainties, could be used to challenge microscopic causality and search for acausal signatures at the LHC.

DOI: https://doi.org/10.18272/aci.v15i1.2780

ACKNOWLEDGMENT

We gratefully acknowledge Edgar Carrera PhD. for his unsurpassable participation, guidance, and aid during this whole investigation. In the same way, we thank Santiago Paredes PhD for his technical assistance. We thankfully recognize the support from the University San Francisco de Quito and PoliGrants - HUBI Project 17462, for the financial assistance in this masteral program.

CONFLICT OF INTERESTS

The authors declare that they have no conflicts of interest to declare.

DOI: https://doi.org/10.18272/aci.v15i1.2780

aci avances en ciencias e ingenierías

REFERENCES

[1] Evans, L., & Bryant, P. (2008). LHC machine. *Journal of Instrumentation, 3*(08), S08001–S08001. doi: https://doi.org/10.1088/1748-0221/3/08/s08001

[2] Quigg, C. (2004). Nature's Greatest Puzzles. *eConf, C040802*, L001. arXiv: https://arxiv.org/abs/hep-ph/0502070

[3] Grinstein, B. [Benjamin], O'Connell, D., & Wise, M. B. (2008). The Lee-Wick standard model. *Phys. Rev. D, 77*, 025012. doi: https://doi.org/10.1103/PhysRevD.77.025012. arXiv: https://arxiv.org/abs/0704.1845 [hep-ph]

[4] Lee, T. D., & Wick, G. C. (1970). Finite theory of quantum electrodynamics. *Phys. Rev. D, 2*, 1033– 1048. doi: https://doi.org/10.1103/PhysRevD.2.1033

[5] Lee, T. D., & Wick, G. C. (1969). Negative Metric and the Unitarity of the S Matrix. *Nucl. Phys. B, 9,* 209–243. doi: https://doi.org/10.1016/0550-3213(69)90098-4

[6] Grinstein, B. [Benjamin], O'Connell, D., & Wise, M. B. (2009). Causality as an emergent macroscopic phenomenon: The lee-wicko(n)model. *Physical Review D, 79*(10). doi: https://doi.org/10.1103/physrevd.79. 105019

[7] Alvarez, E., Da Rold, L., Schat, C., & Szynkman, A. (2009). Vertex Displacements for Acausal Particles: Testing the Lee-Wick Standard Model at the LHC. *JHEP, 10*, 023. doi: https://doi.org/10.1088/1126-6708/2009/ 10/023. arXiv: https://arxiv.org/abs/0908.2446 [hep-ph]

[8] Chatrchyan, S. [S.] et al. (2008). The CMS Experiment at the CERN LHC. *JINST, 3,* S08004. doi: https://doi.org/10.1088/1748-0221/3/08/S08004

[9] Wolfram Research Inc. (n.d.). Mathematica, Version 12.3.1. Champaign, IL, 2021. Retrieved from https://www.wolfram.com/mathematica

[10] Alloul, A., Christensen, N. D., Degrande, C., Duhr, C., & Fuks, B. (2014). Feynrules 2.0 — a complete toolbox for tree-level phenomenology. *Computer Physics Communications, 185*(8), 2250– 2300. doi: https://doi.org/10.1016/j.cpc.2014.04.012

[11] Alwall, J., Herquet, M., Maltoni, F., Mattelaer, O., & Stelzer, T. (2011). Madgraph 5: Going beyond. *Journal of High Energy Physics, 2011*(6). doi: https://doi.org/10.1007/jhep06(2011)128

[12] Sjöstrand, T., Ask, S., Christiansen, J. R., Corke, R., Desai, N., Ilten, P., . . . Skands, P. Z. (2015). An introduction to pythia 8.2. *Computer Physics Communications, 191*, 159–177. doi: https://doi.org/10.1016/j. cpc.2015.01.024

[13] CMS-collaboration. (2016). CMS Software Version 5 3 X (CMSSW 5 3 X) (Version 2.3.X). doi: https://doi.org/10.7483/OPENDATA.CMS.WYJG.FYK9

[14] Edgar Carrera, E. U., Cesar Montero. (n.d.). Examples for event generation with 2012 cmssw machinery. Available at https://opendata.cern.ch/record/12052 (2022).

[15] CMS-collaboration. (2017a). Doublephoton primary dataset in aod format from run of 2012. *Open Data Portal*. doi: https://doi.org/10.7483/OPENDATA.CMS.CEPG.EXLP

[16] CMS-collaboration. (2017b). Doublephoton primary dataset in aod format from run of 2012. *Open Data Portal*. doi: https://doi.org/10.7483/OPENDATA.CMS.KT69.ANB8

[17] CMS-collaboration. (2017c). Simulated dataset dyjetstoll m-50 tunez2star 8tev-madgraph-tarball in aod- sim format for 2012 collision data. *Open Data Portal*. doi: https://doi.org/10.7483/OPENDATA.CMS.ARKO. 6NV3

[18] CMS-collaboration. (2017d). Simulated dataset ttbar 8tev-madspin amcatnlo-herwig in aodsim format for 2012 collision data. *Open Data Portal*. doi: https://doi.org/10.7483/OPENDATA.CMS.XH95.JNSE

[19] CMS-collaboration. (2017e). Simulated dataset w1jetstolnu tunez2star 8tev-madgraph in aodsim format for 2012 collision data. *Open Data Portal*. doi: https://doi.org/10.7483/OPENDATA.CMS.REHM.JKUH

[20] CMS-collaboration. (2017f). Simulated dataset w2jetstolnu tunez2star 8tev-madgraph in aodsim format for 2012 collision data. *Open Data Portal*. doi: https://doi.org/10.7483/OPENDATA.CMS.DELK.2V7R

[21] CMS-collaboration. (2017g). Simulated dataset w3jetstolnu tunez2star 8tev-madgraph in aodsim format for 2012 collision data. *Open Data Portal*. doi: https://doi.org/10.7483/OPENDATA.CMS.HHCJ.TVXH

DOI: https://doi.org/10.18272/aci.v15i1.2780

[22] Chatrchyan, S. [Serguei] et al. (2013). Search in Leptonic Channels for Heavy Resonances Decaying to Long-Lived Neutral Particles. *JHEP, 02*, 085. doi: https://doi.org/10.1007/JHEP02(2013)085. arXiv: https://arxiv.org/abs/1211.2472 [hep-ex]

[23] CMS-collaboration. (2012). Evidence for a new state decaying into two photons in the search for the standard model Higgs boson in pp collisions.

[24] Khachatryan, V. et al. (2017). Search for R-parity violating supersymmetry with displaced vertices in proton-proton collisions at $\sqrt{s} = 8$ TeV. *Phys. Rev. D, 95*(1), 012009. doi: https://doi.org/10.1103/PhysRevD.95.012009. arXiv: https://arxiv.org/abs/1610.05133 [hep-ex]

 DOI: https://doi.org/10.18272/aci.v15i1.2780